Stereospecific Amyloid-like Fibril Formation by a Peptide Fragment of β_2-Microglobulin†

Hiromasa Wadai,‡ Kei-ichi Yamaguchi,‡ Satoshi Takahashi,‡ Takashi Kanno,§ Tomoji Kawai,§ Hironobu Naiki,|| and Yuji Goto*,‡

Institute for Protein Research, Osaka University, and CREST, Japan Science and Technology Agency, Yamadaoka 3-2, Suita, Osaka 565-0871, Japan, Institute of Scientific and Industrial Research, Osaka University, Mihogaoka, Ibaraki, Osaka 567-0047, Japan, and Department of Pathological Sciences, Faculty of Medical Sciences, University of Fukui, and CREST, Japan Science and Technology Agency, Matsuoka, Fukui 910-1193, Japan

Received July 4, 2004; Revised Manuscript Received October 17, 2004

ABSTRACT: Understanding the role of the L/D-stereospecificity of amino acids is important in obtaining further insight into the mechanism of the formation of amyloid fibrils. β_2-Microglobulin is a major component of amyloid fibrils deposited in patients with dialysis-related amyloidosis. A 22-residue peptide of β_2-microglobulin, Ser20−Lys41 (L-K3 peptide), obtained by digestion with *Acromobacter* protease I, formed amyloid-like fibrils in 50% (v/v) 2,2,2-trifluoroethanol and 10 mM HCl at 25 °C, as confirmed by thioflavin T fluorescence, circular dichroism spectra, and atomic force microscopy images. A synthetic K3 peptide composed of D-amino acids (D-K3 peptide) formed similar fibrils but with opposite chirality as indicated by circular dichroism spectra. A mixture of L-K3 and D-K3 peptides also formed fibrils, although the L- and D-amino acid composition of each fibril is unknown. To examine the possible cross-reactivity between L- and D-enantiomers, we carried out seeding experiments in which preformed seeds were extended by monomers. The results revealed that only the homologous extensions proceed smoothly, i.e., the growth of L-seeds by L-monomers or D-seeds by D-monomers. The results suggest that, while the fibrils derived from L- and D-peptides form in a similar manner but with opposite stereochemistry, a cross-reaction between them is prevented because the geometry of the mixed sheet cannot satisfy dominant factors for β-sheet stabilization.

Amyloid fibrils are recognized as being associated with the pathology of more than 20 serious human diseases, and peptides or proteins specific to these diseases have been identified (*1*−*6*). Moreover, various proteins and peptides that are not related to diseases can also form amyloid-like fibrils, implying that the formation of amyloid fibrils is a generic property of polypeptides (*7*−*10*). Irrespective of protein species, electron microscopy and X-ray fiber diffraction indicate that the amyloid fibrils have a relatively rigid and straight morphology consisting of several layers of cross-β-sheets (*11*−*13*). A structural study using solid-state nuclear magnetic resonance spectroscopy has shown that amyloid fibrils are stabilized by juxtaposing hydrophobic segments minimizing electrostatic repulsion (*14*). From the hydrogen−deuterium exchange of amide protons, amyloid fibrils are shown to be stabilized by an intensive network of hydrogen bonds substantiating β-sheets (*15*−*17*). On the basis of various approaches described above, increasingly convincing structural models of amyloid fibrils are emerging. One of the most prevalent arguments is that the amyloid fibril is a supramolecular structure composed of several protofilaments wound around each other, mostly in a left-handed manner (*1*−*6*). The protofilaments themselves probably consist of several layers of a cross-β-sheet structure associated at a distance of 10−15 Å, where the distance between the polypeptide chains in the cross-β-sheet is 4.7 Å. A detailed fold has been proposed for some proteins and peptides in the protofilament, including insulin (*13*) and Aβ (*14*). However, the mechanism of amyloid fibril formation is still far from clear.

With Alzheimer's amyloid β-peptide and its fragments, amyloid fibril formation has been suggested to be a stereospecific reaction (*18*−*20*). It has been reported that, although there was no difference in the amyloid forming properties and fibril morphologies of L- and D-enantiomers made of L- and D-amino acids, respectively, one enantiomer does not cross-react with the other. However, the generality of this observation for other amyloidogenic proteins and peptides is not established. Since configurations of side chains of Ile and Thr with chiral centers are the same in the L- and D-amino acids, L- and D-enantiomers containing these amino acids are not exact mirror images of each other. Therefore, if the role of side chains is important, it is possible that the fibrils formed by L/D-enantiomers are distinct. Details about the stereospecificity of fibril formation will provide important insight into amyloid fibrils.

† This work was supported in part by grants-in-aid for scientific research from the Japanese Ministry of Education, Culture, Sports, Science and Technology on Priority Areas (Grant 40153770) and Scientific Research (B) (Grant 13480219).

* To whom correspondence should be addressed: Institute for Protein Research, Osaka University, Yamadaoka 3-2, Suita, Osaka 565-0871, Japan. Phone: +81-6-6879-8614. Fax: +81-6-6879-8616. E-mail: ygoto@protein.osaka-u.ac.jp.

‡ Osaka University and CREST.

§ Institute of Scientific and Industrial Research, Osaka University.

|| University of Fukui and CREST.

10.1021/bi0485880 CCC: $30.25 © 2005 American Chemical Society
Published on Web 12/04/2004

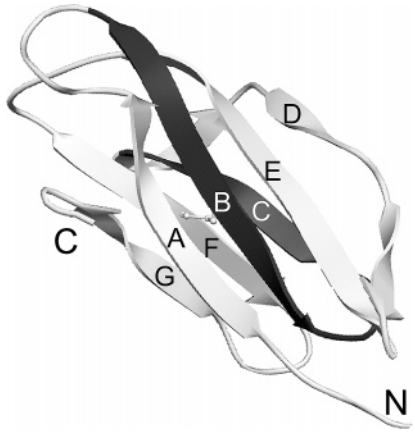

FIGURE 1: Structure of β2-m and amino acid sequence of the K3 peptide. The region corresponding to the K3 peptide is shaded. The diagram was created using Swiss-Pdb Viewer (*46*) with PDB entry 3HLA reported by Bjorkman *et al.* (*23*). The amino acid sequence of the K3 region is Ser20-Asn-Phe-Leu-Asn-Cys-Tyr-Val-Ser-Gly-Phe-His-Pro-Ser-Asp-Ile-Glu-Val-Asp-Leu-Leu-Lys41.

Dialysis-related amyloidosis is a common and serious complication in patients receiving long-term hemodialysis for more than 10 years (*21*, *22*), in which β_2-microglobulin (β2-m)[1] forms amyloid fibrils. Native β2-m, made of 99 amino acid residues, corresponds to a typical immunoglobulin domain (Figure 1) and is a component of the type I major histocompatibility antigen (*23*, *24*). Although an increase in the β2-m concentration in blood over a long period is recognized as the most critical risk factor causing amyloidosis, the molecular details remain unknown. Recently, β2-m, because of its relatively small size which makes it suitable for physicochemical studies, has been used as a target for extensive studies addressing the mechanism of amyloid fibril formation in the context of protein conformation (*25*−*33*). We have been studying the conformation and formation of amyloid fibrils derived from β2-m (*34*−*41*) on the basis of the seed-dependent fibril extension reaction established by Naiki *et al.* (*22*).

In many amyloidogenic proteins, short peptides called minimal or essential sequences can form amyloid fibrils by themselves (*17*, *29*, *41*−*45*). We found that a 22-residue K3 peptide, Ser20−Lys41 (Figure 1), obtained by digestion of β2-m with *Acromobacter* protease I, forms fibrils similar to the amyloid fibrils of the whole β2-m molecule (*34*). It was also found that, while the efficient formation of fibrils by whole β2-m at pH 2.5 requires seeding, the K3 peptide can form amyloid fibrils spontaneously with an optimum at neutral pH, implying that the K3 peptide corresponds to the initiation site or core region of the fibrils formed by whole β2-m (*40*, *41*). In this paper, we show that the K3 peptide forms a fibrillar structure in the presence of a relatively high concentration [50% (v/v)] of 2,2,2-trifluoroethanol (TFE). We consider that the fibrillar structure of the K3 peptide formed in TFE is similar to the protofilament of β2-m in water.

To address the issue of stereospecificity in the formation of amyloid fibrils, we compared the fibrils produced by L- and D-K3 peptides in 50% (v/v) TFE using ThT fluorescence, CD, and AFM. The results show that fibrils made from L- and D-peptides form in a similar manner, although a slightly decreased rate was noted for the D-peptide, and that no cross-reaction occurs between L- and D-peptides, revealing the importance of stereospecificity in fibril formation.

EXPERIMENTAL PROCEDURES

Recombinant β2-m and K3 Peptide. Recombinant human β2-m was expressed in the methylotropic yeast *Pichia pastoris* and purified as described previously (*34*, *35*). The L-K3 peptide was obtained by digestion of β2-m with lysyl endopeptidase from *Achromobacter lyticus* as described previously (*34*, *35*) and purified by reverse phase high-performance liquid chromatography. The D-K3 peptide was purchased from Peptide Institute, Inc. (Osaka, Japan), its purity being >95% according to the elusion pattern from high-performance liquid chromatography. The L-K3 peptide was also purchased from Peptide Institute, Inc., and was indistinguishable from the L-K3 peptide purified from β2-m with respect to fibril formation.

Fibril Formation. D/L-K3 peptides were first dissolved in 50% (v/v) TFE and 10 mM HCl at a final K3 concentration of 200 μM and then incubated at 25 °C. The protein solution was not agitated during the incubation. The conformational change was monitored using ThT fluorescence, CD, and AFM. For the seeding experiments, D- or L-K3 peptides were first dissolved in 10 mM NaOH, since the spontaneous formation of fibrils was slower than that in the K3 solutions directly dissolved in 50% (v/v) TFE and 10 mM HCl. The seed fibrils (i.e., preformed fibrils) were added at a final concentration of 10 μM to 100 μM monomeric K3 in 50% (v/v) TFE and 10 mM HCl at 25 °C. It is noted that the seed concentration is represented by monomer K3 in the seeds.

ThT Fluorescence Assay. The polymerization reaction was monitored by fluorometric analysis with ThT at 25 °C as described previously (*22*, *34*). The excitation and emission wavelengths were 445 and 485 nm, respectively. From each reaction tube, 5 μL was taken and mixed with 1.0 mL of 5 μM ThT in a 50 mM glycine-NaOH buffer (pH 8.5) and the fluorescence of ThT was measured using a model F4500 Hitachi fluorescence spectrophotometer. We confirmed that the ThT assay is not affected significantly by the addition of a low concentration of TFE.

AFM and CD Measurements. A 10 μL sample drop was spotted on freshly cleaved mica. After standing on the substrate for 1 min, the solution was blown off with compressed air and air-dried. AFM images were obtained using a dynamic force microscope (Nanoscope IIIa, Digital Instruments/Veeco). The scanning tip was a Si microcantilever (Digital Instruments/Veeco, spring constant of 40 N/m, resonance frequency of 300 kHz). The protein concentration was 62.5 μg/mL, and the scan rate was 1 Hz.

Far-UV CD spectra were measured with a J-600 Jasco spectropolarimeter at 25 °C using a cell with a light path of 1 mm. The peptide concentration was 40 μM, and the results are expressed as the mean residue ellipticity [θ] (degrees per square centimeter per decimole).

Structural Model of Amyloid Fibrils. Molecular models of the β-sheet were drawn on Swiss-Pdb Viewer (*46*). The parallel β-sheet region in the crystal structure (PDB entry

[1] Abbreviations: AFM, atomic force microscopy; β2-m, β_2-microglobulin; CD, circular dichroism; DMSO, dimethyl sulfoxide; HFIP, 1,1,1,3,3,3-hexafluoro-2-propanol; K3 peptide, 22-residue peptide of β2-m; ThT, thioflavin T; TFE, 2,2,2-trifluoroethanol.

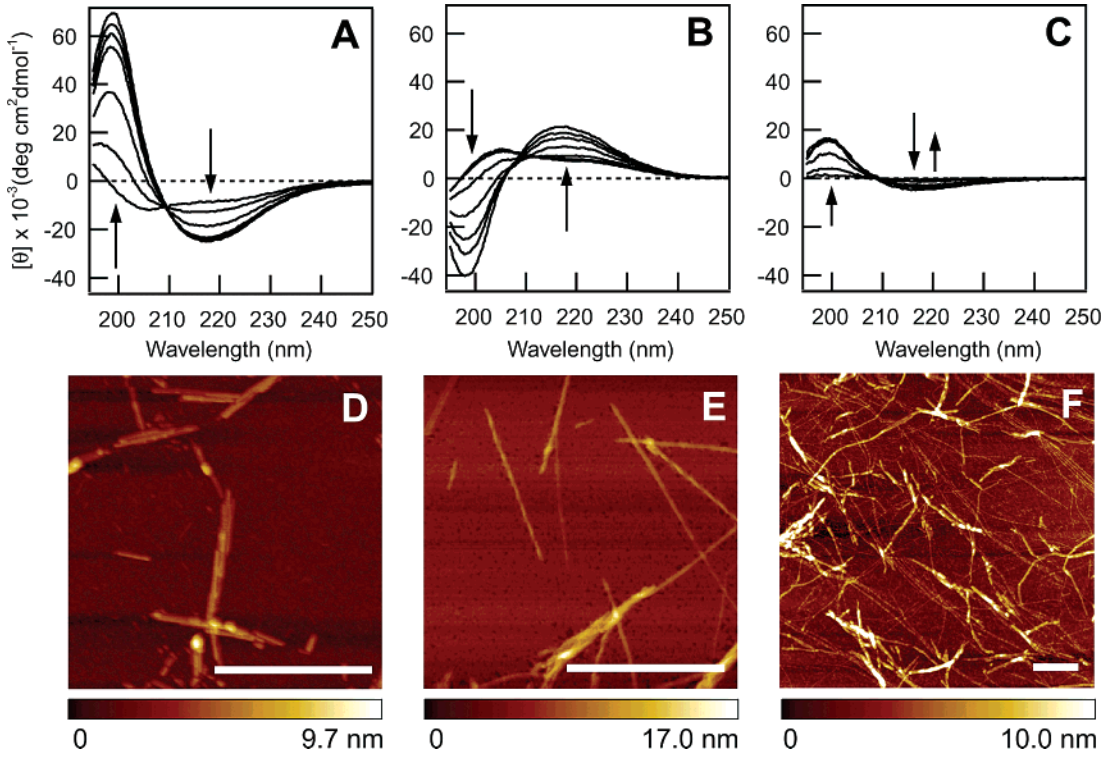

FIGURE 2: Formation of fibrils by L- and D-K3 peptides in 50% (v/v) TFE and 10 mM HCl at 25 °C. CD spectra (A−C) and AFM images (D−F) of L-K3 (A and D), D-K3 (B and F), and a mixture of D- and L-K3 (C and F) are shown. The CD spectra were measured 30 min, 2 h, 56 h, and ~6 weeks after the initiation of incubation. AFM images are after incubation for 48 h (D), 12 days (E), and 1 week (F). The scale bars in the images indicate a length of 0.5 μm. The scales on the bottom represent the height of pixels in the image.

1AIR) of pectate lyase C (*47*) with a strong left-handed twist was used as a template to emphasize the role of twist. The side chains of Asn21−Val27 of L-K3 peptide assuming β-strand in the native β2-m were grafted onto the regions of Asp176−Val182, Asn203−Val209, Asn225−Val231, and Asn248−Val254 of pectate lyase C, forming the parallel β-sheet. The β-sheet made of D-peptides was prepared by making a mirror image of the L-β-sheet. We performed energy minimization on the L- and D-β-sheets with Swiss-Pdb Viewer, but not on the L/D-mixed β-sheets.

RESULTS

Spontaneous Fibril Formation in TFE. The L-K3 peptide forms amyloid fibrils under various pH conditions with an optimum at pH ~6.0 (*40*). This implies that, although the seed-dependent formation by whole β2-m reaches a maximum at pH 2.5 because of the folded conformation at neutral pH, whole β2-m once denatured can reveal an intrinsic propensity to form fibrils at neutral pH. Here, we found that, in the presence of a high concentration of TFE, the L-K3 peptide forms a fibrillar structure similar to the L-K3 amyloid fibrils generated under aqueous conditions (Figure 2A,D). Amyloid fibril formation in TFE has also been reported by others (*48*, *49*).

TFE is an alcohol with a strong potential to induce an α-helical conformation in proteins and unfolded peptides (*50*). Consistent with this, in the presence of 50% (v/v) TFE, the L-K3 peptide first exhibited a CD spectrum indicating an α-helical conformation with a helical content of ~30% estimated by the method of Chen *et al*. (*51*) (Figure 2A). Upon incubation at 25 °C without agitation, the spectrum changed to that of a typical β-sheet structure with a maximum at 218 nm. The presence of an isodichroic point suggests that the transition is approximated by a two-state process between the α-helical and β-sheet states. The reaction occurred without a lag phase and reached saturation at ~50 h with a half-time of 5 h (Figure 3A).

The conformational change in the L-K3 peptide in 50% (v/v) TFE was accompanied by an increase in ThT fluorescence (Figure 3B), a typical characteristic of amyloid fibrils (*22*). The time course of the increase in ThT fluorescence was similar to the conformational change monitored by CD at 218 nm, suggesting that both CD and ThT fluorescence detected the formation of amyloid-like structures. In fact, AFM measurements of the samples incubated in TFE revealed fibrillar structures with a height of 3.0−6.0 nm and a length of 200 nm to 1 μm (Figure 2D). The width of fibrils obtained from the AFM images was smaller than the width of thick amyloid fibrils of L-K3 or intact β2-m (10−15 nm) but is similar to that (~5 nm) of the thinner fibrils of the L-K3 peptide prepared under aqueous conditions (*40*). It is noted that, under aqueous conditions, L-K3 produced several kinds of fibrils with a distinct width (*40*). Similar observations that TFE induces thinner protofilaments whereas mature fibrils are formed under aqueous conditions were reported for the HypF N-terminal domain (*48*).

The measurements described above were also carried out with the D-K3 peptide. As expected, but quite intriguingly, the CD spectrum in 50% (v/v) TFE immediately after dissolution exhibited maxima at ~225 and ~210 nm, indicative of an α-helical conformation with chirality opposite from that of the usual consisting of L-amino acids (Figure 2B). Upon incubation at 25 °C, the spectrum transformed to that with a maximum at 218 nm, showing

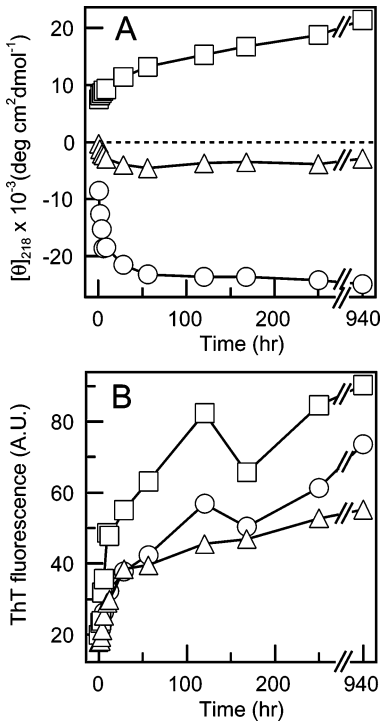

FIGURE 3: Time course of fibril formation by L- and D-K3 peptides in 50% (v/v) TFE and 10 mM HCl at 25 °C. The CD intensity at 218 nm (A) and ThT fluorescence (B) are plotted against the incubation time for 0.2 mM L-K3 (○), 0.2 mM D-K3 (□), and a mixture of 0.1 mM L-K3 and 0.1 mM D-K3 (△).

the formation of a β-sheet with chirality opposite from that of the L-K3 peptide. The time course of the spectral change measured from the ellipticity at 218 nm showed that the reaction was slower than that of the L-K3 peptide (Figure 3A). ThT fluorescence increased notably more than that for the L-K3 peptide, although the reason is unknown. AFM revealed that fibrils similar to those formed by L-K3 are produced (Figure 2E). These results indicated that both L- and D-peptides formed similar fibrils made of β-sheets, but with opposite chirality.

Fibril Formation of a Mixture of L/D-K3 Peptides. We then incubated a mixture of 100 μM L- and 100 μM D-K3 peptides. First, the CD spectrum exhibited a slight increase in intensity at ~220 and ~200 nm. Then, the intensity slowly decreased, resulting in a flat spectrum close to the baseline over the wavelength that was measured (Figures 2C and 3A). Although unusual, the interpretation is straightforward if we assume an additive contribution of L- and D-peptides, where the fibril formation of the former occurs slightly faster than that by the latter. In fact, AFM of a mixture of L- and D-peptides after incubation for 1 week showed many fibrillar structures similar to those of L- and D-peptides (Figure 2F). Moreover, ThT fluorescence increased with time, confirming the formation of amyloid-like structures (Figure 3B).

Cross-Reaction. Although we observed fibril formation by a mixture of L- and D-peptides, it is difficult to distinguish the fibrils made of L- or D-peptides. The observed fibrils might be a mixture of structures formed independently by the L- and D-peptides. Alternatively, each fibril may be made of both L- and D-peptides. Distinguishing between these possibilities is important in clarifying the role of stereospecificity in fibril formation. One way to address this issue is to conduct seeding experiments in which cross-reactions between seeds and monomers are examined.

To focus the effects of seeding, it is preferable to suppress the spontaneous formation of fibrils as much as possible. We found that spontaneous fibril formation was retarded if the K3 peptides were first dissolved in 10 mM NaOH (pH 12). The K3 peptide has three positive (i.e., the α-amino group, His31, and Lys41) and five negative (i.e., Cys25, Asp34, Glu36, Asp38, and the α-carboxyl group) titratable groups, and its isoelectric point calculated on the basis of their pK_a values is pH ~4.5. A higher net charge at pH 12 probably resulted in the complete dissolution of the K3 peptide, consequently suppressing spontaneous nucleation for fibril formation even after the transfer of the solution to acidic conditions. After 2 days at 100 μM monomer in 50% (v/v) TFE at pH 2.0, we saw no significant change in the CD spectrum and ThT fluorescence for either L- or D-K3 peptides (Figure 4C,F and Figure 5).

Under the conditions where the spontaneous formation of fibrils was suppressed, the seed fibrils (i.e., preformed fibrils) were added at a final concentration of 10 μM to 100 μM monomers. Using CD (Figures 4 and 5A), we observed dramatic seeding effects for a combination of L-seeds and L-monomers (Figure 4A) or D-seeds and D-monomers (Figure 4E). Seeding effects were also observed by ThT fluorescence (Figure 5B). In other words, a homologous extension between seeds and monomers occurred effectively, producing L- or D-fibrils, while a heterologous extension did not occur. AFM confirmed the specific fibril formation caused by the homologous seeding effects: Figure 4A for a combination of L-seeds and L-monomers and Figure 4E for a combination of D-seeds and D-monomers.

DISCUSSION

Cross-Reactivity of L/D-Peptides. Although amyloid fibril formation has been suggested to be a stereospecific reaction with the amyloid β-peptide and its fragments (*18*−*20*), the generality of this observation for other amyloidogenic proteins and peptides is not established. Moreover, considering the intricate structure of amyloid fibrils, there are several possibilities explaining the stereospecific amyloid formation. To understand the structure of amyloid fibrils, we focused on the interaction of the L- and D-amino acids constituting the fibrils. We chose the K3 peptide derived from β2-m comprising 22 amino acid residues for the convenience of its chemical synthesis. Then, we chose for the experiment 50% (v/v) TFE in 10 mM HCl at 25 °C, because the formation of fibrils occurred reproducibly without notable amorphous aggregation, which is evident from the CD spectral change with an isodichroic point (Figure 2A,B). However, we do not know if the fibrils formed under these conditions are exactly the same as the amyloid fibrils formed under aqueous conditions. We noted that the fibrils which formed in 50% (v/v) TFE tended to depolymerize when the TFE concentration decreased. A similar observation was reported for a peptide derived from the single-layer β-sheet of OspA (*7*). Diameters of the K3 fibrils in TFE estimated from the height of AFM images (3−6 nm) were smaller than those (10−15 nm) of mature fibrils of L-K3 prepared under aqueous conditions (*40*), suggesting that the fibrils formed in TFE correspond to protofilaments. Similar observations

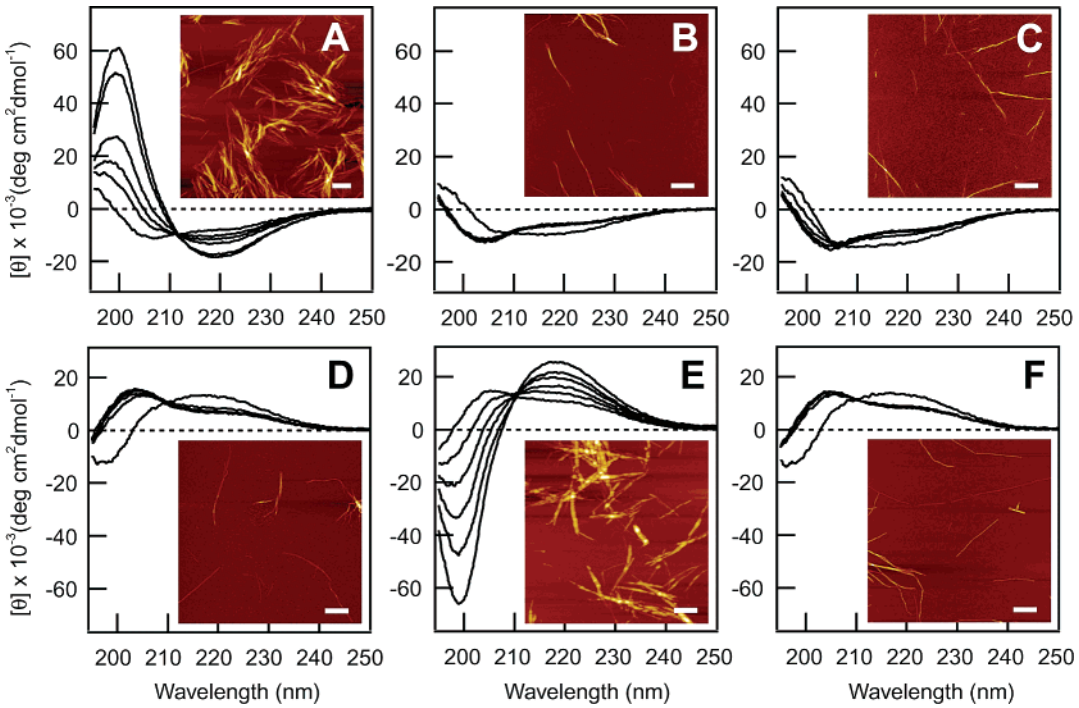

FIGURE 4: Cross-reactions in the formation of amyloid fibrils between L- and D-K3 peptides measured from CD spectra in 50% (v/v) TFE at pH 2.0 and 25 °C. (A−C) Fibril formation of L-K3 in the presence of L-K3 seeds (A) or D-K3 seeds (B) or in the absence of seeds (C). (D−F) Fibril formation of D-K3 in the presence of L-K3 seeds (D) or D-K3 seeds (E) or in the absence of seeds (F). The concentrations of seeds, represented by the monomer K3 concentration, and monomers were 10 and 100 μM, respectively. The CD spectra were recorded 10 min, 12 h, 24 h, 50 h, 100 h, and 1 week after the initiation of incubation. Insets show AFM images of fibrils prepared by incubation for 1 week. The scale bar indicates a length of 0.5 μm.

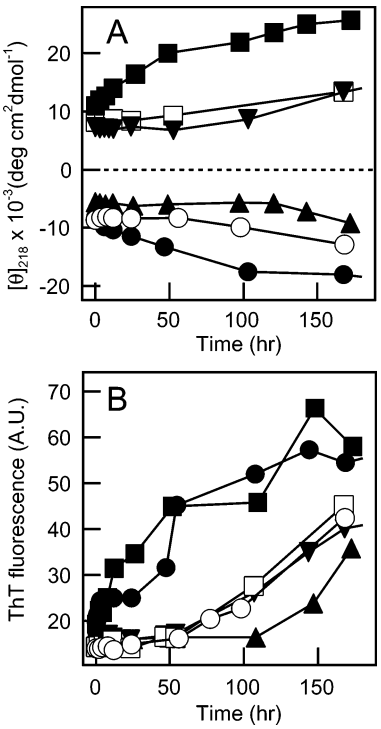

FIGURE 5: Time course of cross-reactions between L- and D-K3 peptides in 50% (v/v) TFE and 10 mM HCl at 25 °C. (A) Time courses measured by CD at 218 nm of fibril formation by L-K3 in the presence of L-K3 seeds (●) or D-K3 seeds (○) or in the absence of seeds (▲) and those of D-K3 in the presence of L-K3 seeds (□) or D-K3 seeds (■) or in the absence of seeds (▼). The values were taken from the spectra shown in Figure 4. (B) Time courses measured by ThT of fibril formation by L-K3 and D-K3. Symbols are the same as in panel A.

that TFE induces thinner protofilaments whereas mature fibrils are formed under aqueous conditions were reported for the HypF N-terminal domain (*48*). Although the fibrils in 50% (v/v) TFE are not exactly the same as mature fibrils, we believe that they are useful for considering the stereospecificity of amyloid fibril formation.

First, we indicated that fibrillization occurs for both L- and D-K3 peptides, leading to apparently similar fibrils, except for the mirror images of CD spectra (Figure 2). However, we noted that the formation is slightly slower with D-K3 than with L-K3 (Figure 3A). This slight but significant difference in the growth rate exists even for a mixture of L- and D-K3 peptides, producing apparently complicated kinetics as monitored by CD (Figures 2C and 3A). The slower rate for the D-K3 peptide is likely to be caused by the difference in the chirality of the side chains, suggesting that the side chain interactions also contribute to the rate of amyloid fibril formation. Importantly, the ThT fluorescence increased in the fibrils formed from both L- and D-peptides, indicating that a specific ordered configuration independent of the L- or D-enantiomer is recognized by ThT (Figure 3B).

Single fibrillar images of amyloid fibrils often exhibit a left-handed spiral (*13*, *37*, *52*, *53*). A β-strand made of L-amino acids has a right-handed twist (Figure 6) (*54*). It is considered that the association of right-handed β-strands produces a left-handed twist in the β-sheet, resulting in the left-handed spiral of amyloid fibrils (*13*). A left-handed twist was observed in the amyloid fibrils of whole β2-m (*37*). However, we could not observe clearly a left-handed spiral in the fibrils made of L-amino acids. Instead, we occasionally observed a right-handed spiral in the fibrils made of D-amino acid residues (Figure 2E). Thus, although we anticipated being able to distinguish the L- and D-amyloid fibrils from

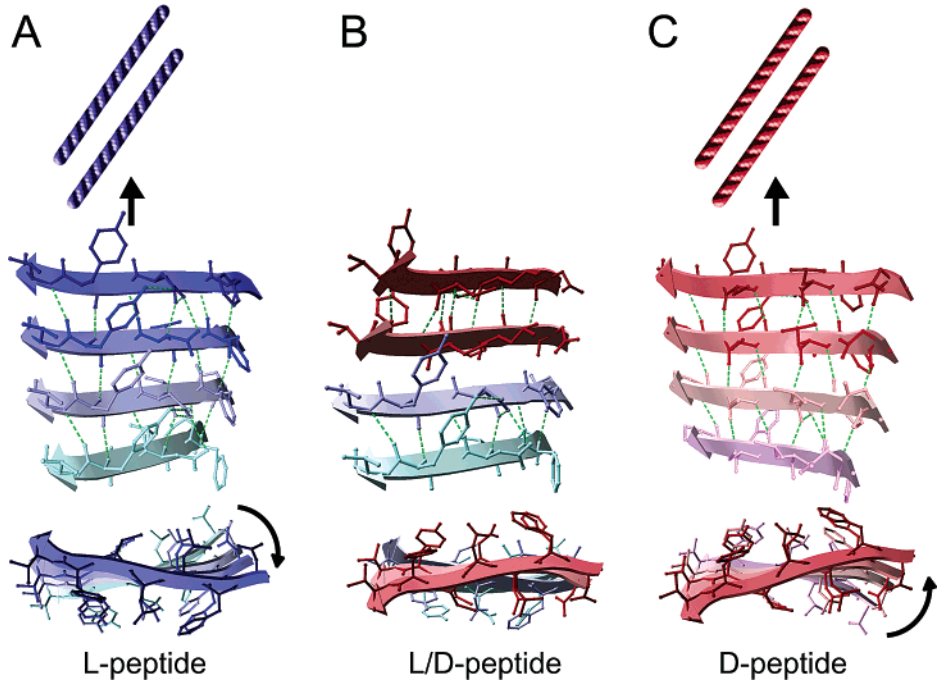

FIGURE 6: Schematic model of fibril formation of peptides made of L-amino acids (A) and D-amino acids (C) and no cross-reactivity of L- and D-peptides (B) in forming amyloid fibrils. (A) A right-handed twist in the β-strand made of L-amino acid residues (colored blue) produces a left-handed twist in the plane of the L-β-sheet, thus forming amyloid fibrils with a left-handed spiral. Green dashed lines represent hydrogen bonds. The bottom image shows a view from the edge of the β-sheet, and the top images show the amyloid fibril. (B) Because of competition over the direction of the β-sheet twist and moreover opposite directions of the side chains, β-sheet made of a mixture of L- and D-β-strands cannot be formed. (C) A left-handed twist in the β-strand made of D-amino acid residues (colored red) produces a right-handed twist in the plane of the D-β-sheet and amyloid fibrils with a right-handed spiral. Schematic models were drawn on Swiss-Pdb Viewer (*46*) by grafting the side chains of Asn21−Val27 of the L-K3 peptide onto the β-sheet region of pectate lyase C (*47*). See Experimental Procedures for details.

the direction of the spiral, this was in fact difficult to do in this work. This difficulty might indeed reflect the decreased extent of spiral in the fibrils made of shorter fragments.

Then, we showed that seeding experiments are useful in examining the possible cross-reaction of L- and D-peptides during fibril formation. The results revealed clearly that only a homologous extension between the seeds and monomers of the same chilarity occurs. The structural modeling of β-sheets made from L- or D-peptides suggests the mechanism with which L- and D-peptides cannot cross-react (Figure 6). A twist of the β-strand as described above implies a simple explanation for why L- and D-peptides do not form chimeric amyloid fibrils. β-Strands made of L- and D-amino acids have right- and left-handed twists, respectively (*54*). The opposite direction of the twists between β-strands of L- and D-peptides may interfere with the formation of persistent hydrogen bonds between them. Moreover, the side chains of residues that are immediately adjacent across the boundary β-strands are on the opposite faces of the β-sheet (Figure 6B). These aspects of geometry of the L/D-chimeric β-sheet are dramatically different from the standard β-sheet geometry so that the chimeric β-sheet cannot simultaneously satisfy dominant factors for β-sheet stabilization, e.g., main chain hydrogen bonds, and hydrophobic, hydrophilic, and van der Waals interactions of side chains. In other words, the inability of L- and D-peptides to form chimeric fibrils arises from fundamental structural properties of the β-sheet; opposite aspects of geometry of the L- and D-β-sheets prevent the tight packing of the polypeptide chain stabilized by persistent hydrogen bonds and side chain interactions. Although we believe there is an important role for β-strand twist, the difficulty in observing clear spirals in AFM images might mean the contributions of other factors are more essential than the β-strand twist.

Fibril Formation in TFE. In this study, we used TFE to produce fibrils of the K3 peptide. It is interesting that TFE, one of the most popular α-helix inducers (*50*), induces fibrils made of β-sheets. A similar observation has been reported for several peptides (*7*, *48*, *49*). Importantly, Chiti *et al.* (*48*) proposed that the assembly of protofilaments into mature amyloid fibrils is guided by the interactions between hydrophobic residues that may remain exposed on the surface of individual protofilaments so that the formation of protofilaments appears to be facilitated in the presence of TFE, a solvent that destabilizes hydrophobic interactions.

The effects of alcohols on proteins and peptides can be explained by nonpolarity or hydrophobicity (*50*, *55*). By intervening in hydrophobic interactions, alcohols tend to denature the native state of proteins or dissociate protein aggregates and amyloid fibrils into monomeric forms. These effects depend on the alcohol species, with the halogenated alcohols, in particular, TFE and HFIP, having marked effects in comparison with methanol or ethanol. We previously proposed that the cluster formation of alcohols explains the marked effects of TFE or HFIP (*50*, *56*). The strong nonpolarity of these alcohols concomitantly strengthens the intramolecular hydrogen bonds as revealed by α-helix formation. This occasionally results in the formation of intermolecular hydrogen bonds, causing aggregation or amyloid fibrils to form. On the other hand, dimethyl sulfoxide, a polar solvent with a strong potential to become a proton acceptor, can always dissolve amyloid fibrils,

although a high concentration is required (*15*, *55*). HFIP or TFE can dissolve amyloid fibrils by weakening hydrophobic interactions. However, this effect is not sufficient to completely dissolve rigid amyloid fibrils. Consequently, depending on the protein species and conditions, a nonpolar environment introduced by alcohols works adversely by strengthening the intermolecular hydrogen bonds, thus inducing amyloid-like fibrils or amorphous aggregates to form. These results indicate that the formation of fibrils is determined by an intricate balance of forces stabilizing and destabilizing the fibrils. Analyzing these factors in detail by taking advantage of the marked effects of alcohols on K3 fragments may help to clarify the mechanism of amyloid fibril formation.

In conclusion, we showed that the D-peptide forms fibrils with stereochemistry opposite from that of the L-peptide. The kinetics of the formation by the D-peptide was similar to that for the L-peptide, although a slight difference was also noted. On the other hand, L- and D-peptides with the same amyloidogenic sequence do not cross-react, consistent with the distinct geometry of L- and D-β-sheets. Therefore, the formation of amyloid fibrils is a highly stereospecific reaction in which the unique chirality of the amino acid residues is required to generate the basic elements (i.e., protofilaments) of the supramolecular structure. Considering these features, it might be possible to design a chimeric amyloidogenic peptide made of L- and D-amino acid residues, in which the L-amino acid residues contribute to binding to the fibril end but the D-amino acid residues prevent the peptide from becoming a template for subsequent growth. Such a chimeric peptide would be useful as a stereospecific inhibitor of amyloid fibril formation.

ACKNOWLEDGMENT

We thank Tomohiko Nakamura for help with the AFM measurements.

REFERENCES

1. Sipe, J. D. (1992) Amyloidosis, *Annu. Rev. Biochem. 61*, 947−975.
2. Rochet, J. C., and Lansbury, P. T., Jr. (2000) Amyloid fibrillogenesis: Themes and variations, *Curr. Opin. Struct. Biol. 10*, 60−68.
3. Serpell, L. C. (2000) Alzheimer's amyloid fibrils: Structure and assembly, *Biochim. Biophys. Acta 1502*, 16−30.
4. Cohen, F. E., and Kelly, J. W. (2003) Therapeutic approaches to protein-misfolding diseases, *Nature 426*, 905−909.
5. Dobson, C. M. (2003) Protein folding and misfolding, *Nature 426*, 884−889.
6. Uversky, V. N., and Fink, A. L. (2004) Conformational constraints for amyloid fibrillation: The importance of being unfolded, *Biochim. Biophys. Acta 1698*, 131−153.
7. Ohnishi, S., Koide, A., and Koide, S. (2000) Solution conformation and amyloid-like fibril formation of a polar peptide derived from a β-hairpin in the OspA single-layer β-sheet, *J. Mol. Biol. 301*, 477−489.
8. Takahashi, Y., Ueno, A., and Mihara, H. (2000) Mutational analysis of designed peptides that undergo structural transition from α-helix to β-sheet and amyloid fibril formation, *Structure 8*, 915−925.
9. Zurdo, J., Guijarro, J. I., Jimenez, J. L., Saibil, H. R., and Dobson, C. M. (2001) Dependence on solution conditions of aggregation and amyloid formation by an SH3 domain, *J. Mol. Biol. 311*, 325−340.
10. López de la Paz, M., Goldie, K., Zurdo, J., Lacroix, E., Dobson, C. M., Hoenger, A., and Serrano, L. (2002) De novo designed peptide-based amyloid fibrils, *Proc. Natl. Acad. Sci. U.S.A. 99*, 16052−16057.
11. Sunde, M., and Blake, C. (1997) The structure of amyloid fibrils by electron microscopy and X-ray diffraction, *Adv. Protein Chem. 50*, 123−159.
12. Serpell, L. C., Sunde, M., Benson, M. D., Tennent, G. A., Pepys, M. B., and Fraser, P. E. (2000) The protofilament substructure of amyloid fibrils, *J. Mol. Biol. 300*, 1033−1039.
13. Jimenez, J. L., Nettleton, E. J., Bouchard, M., Robinson, C. V., Dobson, C. M., and Saibil, H. R. (2002) The protofilament structure of insulin amyloid fibrils, *Proc. Natl. Acad. Sci. U.S.A. 99*, 9196−9201.
14. Tycko, R. (2003) Insight into the amyloid folding problem from solid-state NMR, *Biochemistry 42*, 3151−3159.
15. Hoshino, M., Katou, H., Hagihara, Y., Hasegawa, K., Naiki, H., and Goto, Y. (2002) Mapping the core of the β_2-microglobulin amyloid fibril by H/D exchange, *Nat. Struct. Biol. 9*, 332−336.
16. Kheterpal, I., Lashuel, H. A., Hartley, D. M., Walz, T., Lansbury, P. T., Jr., and Wetzel, R. (2003) Aβ protofibrils possess a stable core structure resistant to hydrogen exchange, *Biochemistry 42*, 14092−14098.
17. Kuwata, K., Matumoto, T., Cheng, H., Nagayama, K., James, T. L., and Roder, H. (2003) NMR-detected hydrogen exchange and molecular dynamics simulations provide structural insight into fibril formation of prion protein fragment 106−126, *Proc. Natl. Acad. Sci. U.S.A. 100*, 14790−14795.
18. Cribbs, D. H., Pike, C. J., Weinstein, S. L., Velazquez, P., and Cotman, C. W. (1997) All-D-enatiomers of β-amyloid exhibit similar biological properties to all-L-β-amyloids, *J. Biol. Chem. 272*, 7431−7436.
19. Shearman, M. S., Ragan, C. I., and Iversen, L. L. (1994) Inhibition of PC12 cell redox activity is a specific, early indicator of the mechanism of β-amyloid-mediated cell death, *Proc. Natl. Acad. Sci. U.S.A. 91*, 1470−1474.
20. Esler, W. P., Stimson, E. R., Fishman, J. B., Ghilardi, J. R., Vinters, H. V., Mantyh, P. W., and Maggio, J. E. (1999) Stereochemical specificity of Alzheimer's disease β-peptide assembly, *Biopolymers 49*, 505−514.
21. Gejyo, F., Yamada, T., Odani, S., Nakagawa, Y., Arakawa, M., Kunitomo, T., Kataoka, H., Suzuki, M., Hirasawa, Y., Shirahama, T., Cohen, A. S., and Schmid, K. (1985) A new form of amyloid protein associated with chronic hemodialysis was identified as β_2-microglobulin, *Biochem. Biophys. Res. Commun. 129*, 701−706.
22. Naiki, H., Hashimoto, N., Suzuki, S., Kimura, H., Nakakuki, K., and Gejyo, F. (1997) Establishment of a kinetic model of dialysis-related amyloid fibril extension *in vitro*, *Amyloid 4*, 223−232.
23. Bjorkman, P. J., Saper, M. A., Samraoui, B., Bennett, W. S., Strominger, J. L., and Wiley, D. C. (1987) Structure of the human class I histocompatibility antigen, HLA-A2, *Nature 329*, 506−512.
24. Verdone, G., Corazza, A., Viglino, P., Pettirossi, F., Giorgetti, G., Mangione, P., Andreola, A., Stoppini, M., Bellotti, V., and Esposito, G. (2002) The solution structure of human β_2-microglobulin reveals the prodromes of its amyloid transition, *Protein Sci. 11*, 487−499.
25. Esposito, G., Michelutti, R., Verdone, G., Viglino, P., Hernández, H., Robinson, C. V., Amoresano, A., Dal Piaz, F., Monti, M., Pucci, P., Mangione, P., Stoppini, M., Merlini, G., Ferri, G., and Bellotti, V. (2000) Removal of the N-terminal hexapeptide from human β_2-microglobulin facilitates protein aggregation and fibril formation, *Protein Sci. 9*, 831−845.
26. McParland, V. J., Kad, N. M., Kalverda, A. P., Brown, A., Kirwin-Jones, P., Hunter, M. G., Sunde, M., and Radford, S. E. (2000). Partially unfolded states of β_2-microglobulin and amyloid formation *in vitro*, *Biochemistry 39*, 8735−8746.
27. Morgan, C. J., Gelfand, M., Atreya, C., and Miranker, A. D. (2001) Kidney dialysis-associated amyloidosis: A molecular role for copper in fiber formation, *J. Mol. Biol. 309*, 339−345.
28. McParland, V. J., Kalverda, A. P., Homans, S. W., and Radford, S. E. (2002) Structural properties of an amyloid precursor of β_2-microglobulin, *Nat. Struct. Biol. 9*, 326−331.
29. Jones, S., Manning, J., Kad, N. M., and Radford, S. E. (2003) Amyloid-forming peptides from β_2-microglobulin: Insights into the mechanism of fibril formation *in vitro*, *J. Mol. Biol. 325*, 249−257.
30. Jones, S., Smith, D. P., and Radford, S. E. (2003) Role of the N- and C-terminal strands of β_2-microglobulin in amyloid formation at neutral pH, *J. Mol. Biol. 330*, 935−941.

31. Kad, N. M., Myers, S. L., Smith, D. P., Alastair Smith, D., Radford, S. E., and Thomson, N. H. (2003) Hierarchical assembly of β_2-microglobulin amyloid *in vitro* revealed by atomic force microscopy, *J. Mol. Biol. 330*, 785−797.
32. Rasano, C., Zuccotti, S., Mangione, P., Giorgetti, S., Bellotti, V., Pettirossi, F., Corazza, A., Viglino, P., Esposito, G., and Bolognesi, M. (2004) β_2-Microglobulin H31Y variant 3D structure highlights the protein natural propensity towards intermolecular aggregation, *J. Mol. Biol. 335*, 1051−1064.
33. Corazza, A., Pettirossi, F., Viglino, P., Verdone, G., Garcia, J., Dumy, P., Giorgetti, S., Mangione, P., Raimondi, S., Stoppini, M., Bellotti, V., and Esposito, G. (2004) Properties of some variants of human β_2-microglobulin and amyloidogenesis, *J. Biol. Chem. 279*, 9176−9189.
34. Kozhukh, G. V., Hagihara, Y., Kawakami, T., Hasegawa, K., Naiki, H., and Goto, Y. (2001) Investigation of a peptide responsible for amyloid fibril formation of β_2-microglobulin by *Acromobacter* protease I, *J. Biol. Chem. 277*, 1310−1315.
35. Ohhashi, Y., Hagihara, Y., Kozhukh, G., Hoshino, M., Hasegawa, K., Yamaguchi, I., Naiki, H., and Goto, Y. (2002) The intrachain disulfide bond of β_2-microglobulin is not essential for the immunoglobulin fold at neutral pH, but is essential for amyloid fibril formation at acidic pH, *J. Biohem. 131*, 45−52.
36. Hong, D. P., Gozu, M., Hasegawa, K., Naiki, H., and Goto, Y. (2002) Conformation of β_2-microglobulin amyloid fibrils analyzed by reduction of the disulfide bond, *J. Biol. Chem. 277*, 21554−21560.
37. Katou, H., Kanno, T., Hoshino, M., Hagihara, Y., Tanaka, H., Kawai, T., Hasegawa, K., Naiki, H., and Goto, Y. (2002) The role of disulfide bond in the amyloidogenic state of β_2-microglobulin studied by heteronuclear NMR, *Protein Sci. 11*, 2218−2229.
38. Ban, T., Hamada, D., Hasegawa, K., Naiki, H., and Goto, Y. (2003) Direct observation of amyloid fibril growth monitored by thioflavin T fluorescence, *J. Biol. Chem. 278*, 16462−16465.
39. Chiba, T., Hagihara, Y., Higurashi, T., Hasegawa, K., Naiki, H., and Goto, Y. (2003) Amyloid fibril formation in the context of full-length protein: Effect of proline mutations on the amyloid fibril formation of β_2-microglobulin, *J. Biol. Chem. 278*, 47016−47024.
40. Ohhashi, Y., Hasegawa, K., Naiki, H., and Goto, Y. (2004) Optimum amyloid fibril formation of a peptide fragment suggests the amyloidogenic preference of β_2-microglobulin under physiological conditions, *J. Biol. Chem. 279*, 10814−10821.
41. Yamaguchi, K., Katou, H., Hoshino, M., Hasegawa, K., Naiki, H., and Goto, Y. (2004) Core and heterogeneity of β_2-microglobulin amyloid fibrils as revealed by H/D exchange, *J. Mol. Biol. 338*, 559−571.
42. MacPhee, C. E., and Dobson, C. M. (2000) Chemical dissection and reassembly of amyloid fibrils formed by a peptide fragment of transthyretin, *J. Mol. Biol. 297*, 1203−1215.
43. Balbach, J. J., Ishii, Y., Antzutkin, O. N., Leapman, R. D., Rizzo, N. W., Dyda, F., Reed, J., and Tycko, R. (2000) Amyloid fibril formation by Aβ 16−22, a seven-residue fragment of the Alzheimer's β-amyloid peptide, and structural characterization by solid-state NMR, *Biochemistry 39*, 13748−13759.
44. Krebs, M. R. H., Wilkins, D. K., Chung, E. W., Pitleathly, M. C., Chamberlain, A. K., Zurdo, J., Robinson, C. V., and Dobson, C. M. (2000) Formation and seeding of amyloid fibrils from wild-type hen lysozyme and a peptide fragment from the β-domain, *J. Mol. Biol. 300*, 541−549.
45. Uversky, V. N., and Fink, A. L. (2002) Amino acid determinants of α-synuclein aggregation: Putting together pieces of the puzzle, *FEBS Lett. 522*, 9−13.
46. Guex, N., and Peitsch, M. C. (1997) SWISS-MODEL and the Swiss-PdbViewer: An environment for comparative protein modeling, *Electrophoresis 18*, 2714−2723.
47. Lietzke, S. E., Scavetta, R. D., Yoder, M. D., and Jurnak, F. (1996) The refined three-dimensional structure of pectate lyase E from *Erwinia chrysanthemi* at 2.2 Å resolution, *Plant Physiol. 111*, 73−92.
48. Chiti, F., Bucciantini, M., Tapanni, C., Taddei, N., Dobson, C. M., and Stefani, M. (2001) Solution conditions can promote formation of either amyloid protofilaments or mature fibrils from HypF N-terminal domain, *J. Protein Sci. 10*, 2541−2547.
49. Li, H.-T., Du, H.-N., Tang, L., Hu, J., and Hu, H.-Yu. (2002) Structural transformation and aggregation of human α-synuclein in trifluoroethanol, *Biopolymers 64*, 221−226.
50. Nakaoka, N., Mizuno, K., and Goto, Y. (1998) Group additive contributions to the alcohol-induced α-helix formation of melittin: Implication for the mechanism of the alcohol effects on proteins, *J. Mol. Biol. 275*, 365−378.
51. Chen, Y.-H., Yang, J. T., and Martinez, H. M. (1972) Determination of the secondary structures of proteins by circular dichroism and optical rotatory dispersion, *Biochemistry 11*, 4120−4131.
52. Goldsbury, C., Kistler, J., Aebi, U., Arvinte, T., and Cooper, G. J. S. (1999) Watching amyloid fibrils grow by time-lapse atomic force microscopy, *J. Mol. Biol. 285*, 33−39.
53. Goldsbury, C. S., Wirtz, S., Müller, S. A., Sunderji, S., Wicki, P., Aebi, U., and Frey, P. (2000) Studies on the in vitro assembly of Aβ1−40: Implications for the search for Aβ fibril formation inhibitors, *J. Struct. Biol. 130*, 213−231.
54. Richardson, J. S. (1981) The anatomy and taxonomy of protein structure, *Adv. Protein Chem. 34*, 167−339.
55. Hirota-Nakaoka, N., Hasegawa, K., Naiki, H., and Goto, Y. (2003) Dissolution of β_2-microglobulin amyloid fibrils by dimethylsufloxide, *J. Biochem. 134*, 159−164.
56. Hong, D.-P., Kuboi, R., Hoshino, M., and Goto, Y. (1999) Clustering of fluorine-substituted alcohols as a factor responsible for their marked effects on proteins and peptides, *J. Am. Chem. Soc. 121*, 8427−8433.

BI0485880